

Research Article

A Comparative Study of the Inhibitory Effect of Gum Exudates from *Khaya senegalensis* and *Albizia ferruginea* on the Corrosion of Mild Steel in Hydrochloric Acid Medium

Paul Ocheje Ameh

Physical Chemistry Unit, Department of Chemistry, Nigeria Police Academy, PMB 3474, Wudil, Kano State, Nigeria

Correspondence should be addressed to Paul Ocheje Ameh; amehpaul99@gmail.com

Received 13 May 2015; Revised 14 October 2015; Accepted 1 November 2015

Academic Editor: Yanqing Lai

Copyright © 2015 Paul Ocheje Ameh. This is an open access article distributed under the Creative Commons Attribution License, which permits unrestricted use, distribution, and reproduction in any medium, provided the original work is properly cited.

A comparative study of the inhibitory potentials of gum exudates from *Albizia ferruginea* (AF) and *Khaya senegalensis* (KS) on the corrosion of mild steel in HCl medium was investigated using weight loss and gasometric method. The active chemical constituents of the gum were elucidated using GC-MS while FTIR was used to identify the bonds/functional groups in the gums. The two gum exudates were found to be good corrosion inhibitors for mild steel in acidic medium. On comparison, maximum inhibition efficiency was found in *Khaya senegalensis* with 82.56% inhibition efficiency at 0.5% g/L concentration of the gum. This may be due to the fact that more compounds with heteroatoms were identified in the GCMS spectrum of KS gum compared to the AF gum. The presence of such compounds may have enhanced their adsorption on the metal surface and thereby blocking the surface and protecting the metal from corrosion. The adsorption of the inhibitors was found to be exothermic and spontaneous and fitted the Langmuir adsorption model.

1. Introduction

Interaction between valuable metals (such as mild steel) and aggressive media (such as acid, base, or salt) is a serious impediment that may risk cost benefit analysis in the operation of some industries [1]. The effects of these on the safe, reliable, and efficient operation of equipment or structures sometimes are often more serious than simple loss of a mass of a metal [2–4]. Several methods have been investigated and implemented to reduce the corrosion process and extend the lifetime of the metals/structures including painting, electroplating, coating, and cathodic protection [5–9]. The use of inhibitors has been found to be one of the best options available for the protection of metals against corrosion [10].

The use of plant products (such as extracts, gums, and latex), as corrosion inhibitors, is also on the increase [11–20]. The greatly expanded interest in these naturally occurring substances is attributed to the fact that they are cheap, readily available, and ecologically friendly and possess no threat to the environment. In addition, they contain compounds that

may be aromatic and rich in π -electrons and suitable functional groups (such as C=C, C=O, and -OH) [21]. Plant gum exudates from *Ferula assa-foetida* [22], *Dorema ammoniacum* [22], *Guar gum* [23], *Raphia hookeri* [18], *Pacchyllobus edulis* [24], and so forth have been reported as good corrosion inhibitors recently because they are less toxic, green, and eco-friendly.

It is also known that Nigeria is rich in many plant gums species which have not been put into use. Current trends in corrosion inhibition researches are directed towards finding inhibitors (green corrosion inhibitors such as gums) that are eco-friendly, less expensive, and biodegradable.

Hence, the present study is aimed at elucidating the chemical structures of *Khaya senegalensis* and *Albizia ferruginea* and evaluating their corrosion inhibition potentials. From the identified chemical constituents or structures that are inherent in the gums, other industrial potentials of the plant were also investigated. The assessment of the corrosion behaviour was studied using weight loss and gasometric techniques while FTIR measurements were used to study

the functional groups associated with the adsorption of the inhibitor.

2. Materials and Methods

2.1. Materials. Corrosion experiments were performed on mild steel specimens with weight percentage composition as follows: Mn (0.6), P (0.36), C (0.15), Si (0.03), and the rest Fe. The sheet was mechanically press-cut into different coupons, each of dimension $5 \times 4 \times 0.11$ cm. These coupons were degreased in absolute ethanol, dried in acetone, and stored in a desiccator free of moisture prior to their use in corrosion studies. The aggressive solutions for gasometric and weight loss studies were 2.5 and 0.1 M, respectively.

Albizia ferruginea (AF) and *Khaya senegalensis* (KS) used as inhibitors were obtained as dried exudates from their parent trees grown at Kanya Babba village in Bubura Local Government Area of Jigawa State, Nigeria, and purified following the method described by Eddy et al. [25]. The concentrations of AF and KS (inhibitors) were prepared and used for the study range from 0.1 g/L to 0.5 g/L.

2.2. GC-MS Analysis. GC-MS analysis was carried out as described by Eddy et al. [25]. Interpretation on mass spectrum GC-MS was conducted using the database of National Institute Standard and Technology (NIST) having more than 62,000 patterns. The spectrum of the unknown component was compared with the spectrum of the known components stored in the NIST library. The name, molecular weight, and structure of the components of the test materials were ascertained. Concentrations of the identified compounds were determined through area and height normalization.

2.3. Corrosion Inhibition Study

2.3.1. Weight Loss Method. The weight loss of the mild steel in 0.1 M HCl with and without the various concentrations of the inhibitors (AF and KS) was determined at 303, 313, 323, and 333 K as described by Oguzie [13]. The coupons were retrieved every 24 hrs for 7 days (168 hrs.) and the difference in weight for a period of 168 hours was taken as total weight loss.

The inhibition efficiency (%I) for each inhibitor was calculated using [25]

$$\%I = \left(1 - \frac{W_1}{W_2}\right) \times 100, \quad (1)$$

where W_1 and W_2 are the weight losses (g/dm^3) for mild steel in the presence and absence of inhibitor in HCl solution, respectively. The degree of surface coverage θ is given by [25]

$$\theta = \left(1 - \frac{W_1}{W_2}\right). \quad (2)$$

The corrosion rates for mild steel corrosion in different concentrations of the acid were determined for 168-hour immersion period from weight loss using [26]

$$\text{Corrosion rate (mpy)} = \frac{534W}{DAT}, \quad (3)$$

where W is weight loss (mg), D is density of specimen (g/cm^3), A is area of specimen (square inches), and T is period of immersion (hour).

2.3.2. Gasometry Method. The reaction vessel and procedure for determining the corrosion behaviour by this method have been described elsewhere [25]. The experiment was performed at 303 and 333 K for different concentrations of HCl (blank), AF, and KS acting as inhibitors. From the results obtained, the corrosion inhibition efficiency was calculated using the following equation:

$$\%IE = \frac{V_b - V_t}{V_b} \times 100, \quad (4)$$

where V_b is the volume of hydrogen gas evolved by the blank and V_t is the volume of hydrogen gas evolved in the presence of the inhibitor, after time, t .

2.4. FTIR Analysis. FTIR analysis of the corrosion product of mild steel and those of the studied gums was carried out at the National Research Institute of Chemical Technology (NARICT), Zaria, Kaduna State, Nigeria, using Shimadzu FTIR-8400S Fourier transform infrared spectrophotometer. The sample was prepared using KBr and the analysis was done by scanning the sample through a wave number range of 400 to 4000 cm^{-1} .

3. Results and Discussions

3.1. GC-MS Study. Chemical structures of most probable compounds deduced from the GC-MS spectra of KS and AF gums are presented in Figures 1 and 2, respectively. The retention time (RT), IUPAC names of the compounds suggested by reliable spectral library, molecular weight (MW), and charge to mass ratio (m/z) are presented in Tables 1 and 2. Since the area under a GC spectrum is proportional to concentration, normalization of area of the peaks was carried out and used for estimation of percentage concentration (%C) of the respective constituents of the gums. Height normalization was also carried out and the concentrations of constituents (%) based on height normalization were comparable to those obtained from area normalization.

The GC-MS spectra of KS gum revealed 18 peaks. However, only 9 peaks were prominent. From the results presented, it is evident that the most abundant compound in KS gum is nerolidol isobutyrate (peak 15), which constituted about 28%.

This compound undergoes fragmentation into six molecular ions and is characterized with a mass peak value of 41. The compound is a fragrance agent and up to 1:10 0000 in the fragrance concentrate is recommended for use [27]. Another major component of KS gum is pinene (line 2: 20.31%), which was separated with characteristic mass peak value of 50 and with about 9 fragment ions. Pinene ($\text{C}_{10}\text{H}_{16}$) is a bicyclic monoterpene. There are two structural isomers of pinene found in nature: α -pinene and β -pinene. As the name suggests, both forms are important constituents of pine resin; they are also found in the resins of many other

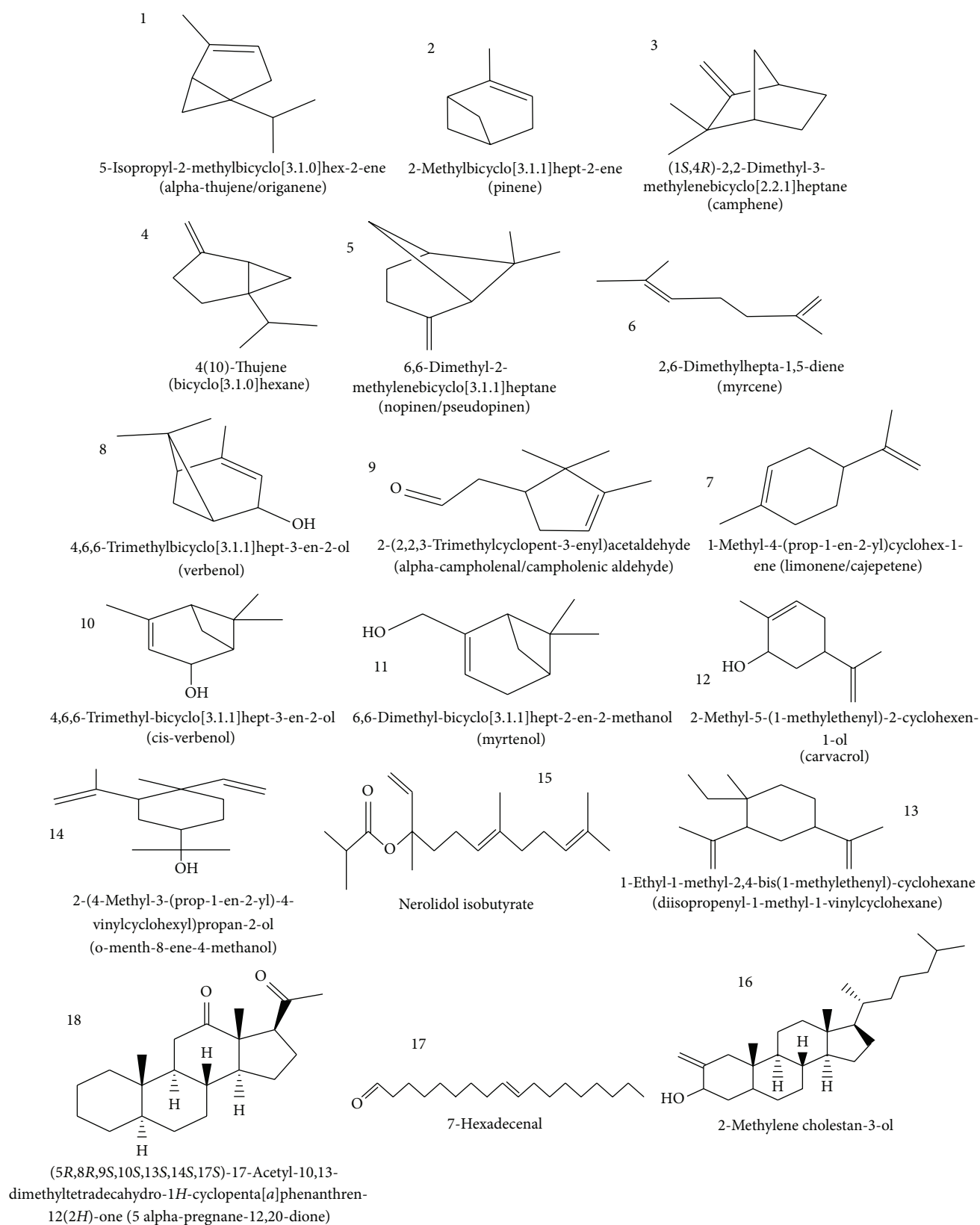


FIGURE 1: Chemical structures of compounds identified in GC-MS spectrum of KS gum (numbering corresponds to the GC line number).

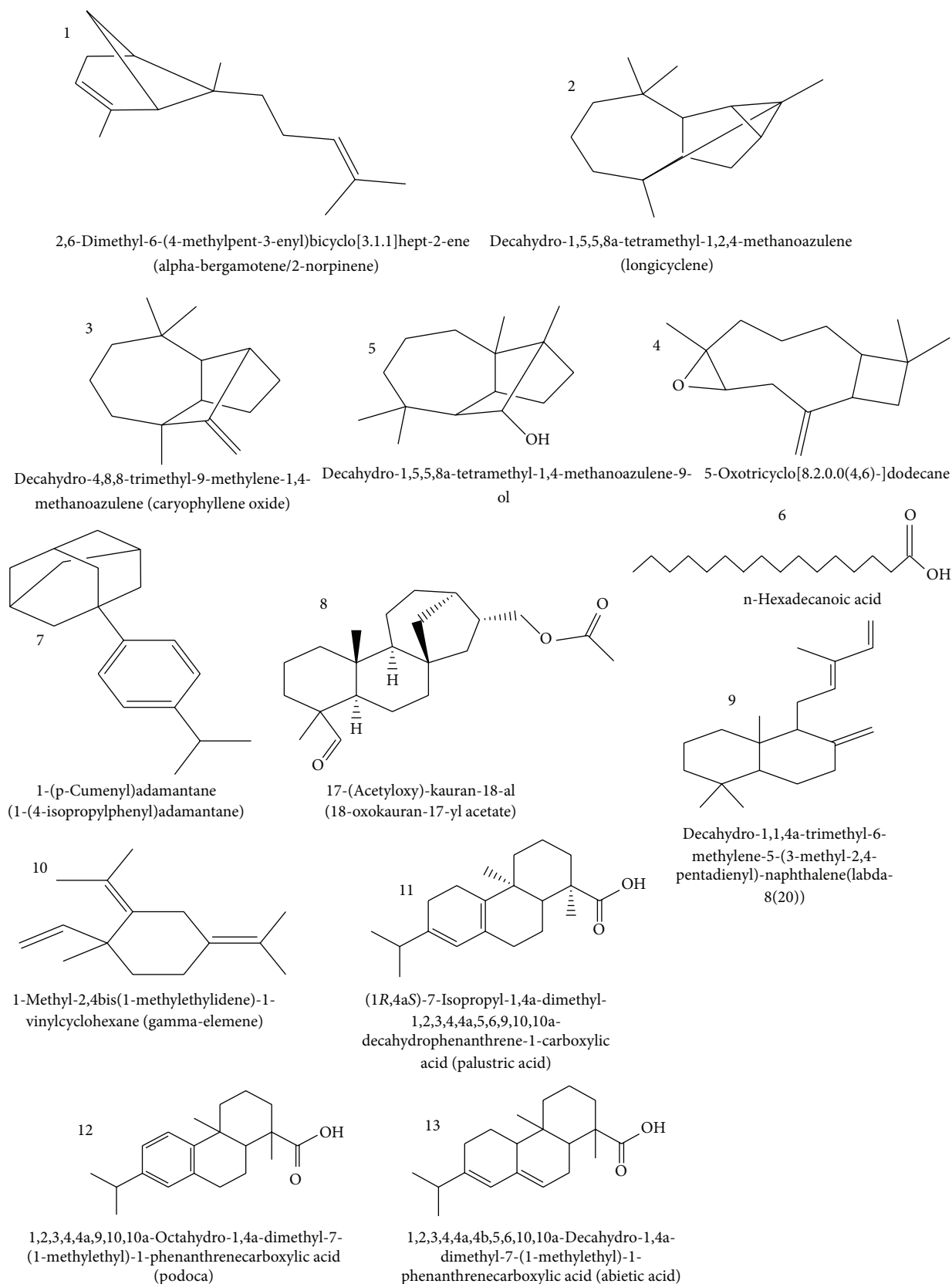


FIGURE 2: Chemical structures of compounds identified in GC-MS spectrum of AF gum (numbering corresponds to the GC line number).

TABLE I: Summary of GC-MS results from peaks in KS gum spectrum.

Line number	%C	Compound	MF	MW	RT	Fragmentation peaks
1	6.22	alpha-Thujene/origanene	C ₁₀ H ₁₆	136	6.9	27 (15%), 41 (15%), 43 (15%), 65 (10%), 77 (50%), 93 (100%), 105 (2%), 121 (2%), and 136 (10%)
2	20.31	Myrcene	C ₁₀ H ₁₆	136	7.1	27 (15%), 41 (20%), 53 (10%), 67 (100%), 77 (35%), 93 (100%), 105 (10%), 121 (20%), and 136 (10%)
3	1.39	Camphene	C ₁₀ H ₁₆	136	7.4	27 (20%), 39 (30%), 53 (20%), 67 (30%), 79 (40%), 93 (100%), 107 (30%), 121 (60%), and 136 (20%)
4	1.90	4(10)-Thujene (bicyclo[3.1.0]hexane)	C ₁₀ H ₁₆	136	8.0	27 (25%), 41 (40%), 43 (15%), 69 (15%), 77 (40%), 93 (100%), 105 (2%), 121 (10%), and 136 (20%)
5	2.61	Nopinen/pseudopinen	C ₁₀ H ₁₆	136	8.1	27 (20%), 41 (60%), 53 (15%), 69 (40%), 77 (30%), 93 (100%), 105 (2%), 121 (15%), and 136 (15%)
6	1.39	2,6-Dimethylhepta-1,5-diene	C ₁₀ H ₁₆	136	8.5	27 (20%), 41 (100%), 53 (20%), 69 (80%), 77 (25%), 93 (100%), 107 (8%), 121 (10%), and 136 (5%)
7	2.37	Limonene/cajepetene	C ₁₀ H ₁₆	136	9.6	27 (40%), 39 (60%), 53 (45%), 68 (100%), 79 (40%), 93 (65%), 107 (20%), 121 (20%), and 136 (25%)
8	3.01	Verbenol	C ₁₀ H ₁₆ O	152	11.6	27 (35%), 41 (65%), 43 (40%), 59 (55%), 79 (60%), 94 (100%), 109 (90%), 119 (30%), and 137 (20%)
9	1.14	alpha-Campholenal	C ₁₀ H ₁₆ O	152	12.0	27 (15%), 39 (20%), 55 (20%), 67 (25%), 81 (20%), 93 (55%), 108 (100%), 119 (5%), 137 (2%), and 152 (2%)
10	7.24	cis-Verbenol	C ₁₀ H ₁₆ O	152	12.8	27 (35%), 41 (60%), 43 (40%), 59 (50%), 79 (60%), 94 (100%), 109 (100%), 119 (30%), and 137 (20%)
11	2.61	Myrtenol	C ₁₀ H ₁₆ O	152	14.3	27 (20%), 41 (40%), 43 (20%), 67 (20%), 79 (100%), 91 (50%), 108 (40%), 119 (30%), 134 (20%), and 152 (10%)
12	0.67	Carvacrol	C ₁₀ H ₁₆ O	152	14.8	27 (10%), 41 (32%), 55 (35%), 69 (20%), 83 (30%), 84 (55%), 109 (100%), 119 (20%), 137 (10%), and 152 (10%)
13	2.91	Diisopropenyl-1-methyl-1-vinylcyclohexane	C ₁₅ H ₂₄	204	31.8	27 (32%), 41 (100%), 53 (60%), 68 (100%), 81 (100%), 93 (80%), 107 (40%), 121 (35%), 133 (15%), 147 (20%), 161 (15%), and 189 (15%)
14	8.44	o-Menth-8-ene-4-methanol	C ₁₅ H ₂₆ O	222	33.2	27 (12%), 39 (18%), 43 (38%), 59 (100%), 81 (50%), 93 (70%), 107 (40%), 121 (30%), 135 (22%), 147 (10%), 161 (40%), 189 (20%), and 204 (10%)
15	28.82	Nerolidol isobutyrate	C ₁₉ H ₃₂ O ₂	292	33.3	41 (42%), 43 (100%), 69 (25%), 71 (50%), 93 (30%), 107 (10%), 121 (40%), 127 (5%), 143 (2%), and 161 (2%)
16	6.23	2-Methylene cholestan-3-ol	C ₂₈ H ₄₈ O	400	34.0	65 (10%), 69 (100%), 81 (75%), 95 (70%), 105 (35%), 121 (25%), 133 (15%), 149 (15%), and 161 (10%)
17	0.81	7-Hexadecenal	C ₁₆ H ₃₀ O	238	35.2	41 (80%), 55 (90%), 71 (78%), 85 (50%), 98 (40%), 121 (40%), 135 (20%), and 141 (10%)
18	1.93	5 alpha-pregnane-12,20-dione	C ₂₃ H ₃₆ OS ₂	392	39.9	43 (80%), 67 (25%), 81 (35%), 95 (18%), 105 (20%), 119 (40%), 131 (15%), 145 (20%), 159 (10%), 189 (8%), 203 (5%), 229 (10%), 255 (50%), 299 (10%), 331 (10%), 349 (20%), 350 (4%), 364 (4%), and 392 (100%)

conifers, as well as in nonconiferous plants. In chemical industry, selective oxidation of pinene with catalysts gives many compounds for perfumery, such as artificial odorants.

In line 14, 8.8% of o-menth-8-ene-4-methanol (2-(4-methyl-3-(prop-1-en-2-yl)-4-vinylcyclohexyl)propan-2-ol) was isolated with characteristic mass peak of 128. Eighteen fragmentation ions were identified in the mass spectrum of the sample. In line 10, 7.24% of cis-verbenol (4,6,6-trimethylbicyclo[3.1.1]hept-3-en-2-ol) was identified. The mass peak for this fraction was 63 and 8 fragment ions characterized the mass spectrum. Verbenol is one of the common ingredients in flavour and fragrance. An isomer of verbenol was also identified in line 8 (3.01%) of the spectrum. However, the concentration of this isomer was much lower than that found in line 10. About 6.22% of alpha-thujene/origanene (5-isopropyl-2-methylbicyclo[3.1.0]hex-2-ene) was separated

in line 1 of the GC-MS spectrum of KS. Mass peak for the separated compound was 41 and 7 fragment ions were identified in the mass spectrum. Thujene (or α -thujene) is a natural organic compound classified as a monoterpene. It is found in the essential oils of a variety of plants and contributes pungency to the flavour of some herbs such as Summer savory. The term *thujene* usually refers to α -thujene. A less common chemically related double-bond isomer is known as β -thujene (or 2-thujene). Another double-bond isomer is known as sabinene which is one of the chemical compounds that contributes to the spiciness of black pepper and is a major constituent of carrot seed oil. Thujene has long been known for its fragrance and medicinal functions.

Area normalization of the GC-MS spectrum of line 16 indicated the presence of 6.23% of 2-methylene cholestan-3-ol. This compound is a derivative of cholesterol, an

TABLE 2: Summary of GC-MS results from peaks in AF gum spectrum.

Peak number	%C	Compound	MF	MW	RT	MP	Fragmentation peaks
1	0.27	alpha-Bergamotene	C ₁₅ H ₂₄	204	18.9	42	69 (40%), 77 (35%), 91 (100%), 107 (40%), 119 (90%), 133 (10%), 147 (5%), 161 (15%), 189 (5%), and 204 (5%)
2	0.65	Longicyclene	C ₁₅ H ₂₄	204	19.5	57	27 (20%), 41 (60%), 55 (30%), 69 (25%), 79 (30%), 94 (100%), 105 (60%), 119 (50%), 133 (40%), 147 (35%), 161 (40%), 180 (30%), and 204 (35%)
3	9.15	1,4-Methanoazulene	C ₁₅ H ₂₄	204	20.5	89	27 (35%), 41 (100%), 55 (55%), 67 (40%), 79 (70%), 91 (90%), 107 (70%), 119 (55%), 133 (10%), 149 (10%), 161 (5%), and 177 (5%)
4	1.25	Caryophyllene oxide	C ₁₅ H ₂₄ O	220	26.5	68	27 (25%), 41 (90%), 69 (45%), 81 (40%), 85 (100%), 109 (45%), 119 (45%), 137 (20%), 151 (10%), 161 (15%), 189 (35%), and 204 (40%)
5	0.66	1,4-Methanoazulene-9-ol	C ₁₅ H ₂₆ O	222	26.9	64	27 (10%), 41 (60%), 55 (40%), 69 (45%), 81 (30%), 85 (100%), 109 (45%), 119 (45%), 137 (20%), 151 (10%), 161 (15%), 189 (35%), and 204 (40%)
6	0.64	n-Hexadecanoic acid	C ₁₆ H ₃₂ O ₂	256	31.7	72	27 (20%), 41 (80%), 43 (100%), 60 (90%), 73 (100%), 85 (25%), 98 (20%), 115 (15%), 129 (40%), 143 (5%), 157 (10%), 171 (10%), 185 (10%), 213 (20%), 227 (5%), and 256 (50%)
7	0.45	1-(p-Cumenyladamantane)	C ₁₉ H ₂₆	254	32.5	128	39 (40%), 41 (85%), 67 (15%), 79 (35%), 91 (40%), 105 (20%), 115 (20%), 135 (40%), 145 (10%), 155 (50%), 169 (5%), 197 (20%), 211 (5%), 239 (60%), and 254 (50%)
8	1.38	18-Oxokauran-17-ylacetate	C ₂₂ H ₃₄ O ₃	346	33.3	150	31 (5%), 41 (50%), 43 (100%), 67 (40%), 81 (50%), 91 (35%), 109 (30%), 123 (40%), 135 (10%), 149 (5%), 161 (5%), 187 (5%), 257 (5%), and 286 (10%)
9	1.27	Naphthalene	C ₂₀ H ₃₂	272	33.9	132	27 (15%), 41 (80%), 55 (60%), 69 (55%), 81 (65%), 95 (55%), 105 (50%), 119 (40%), 137 (40%), 149 (20%), 161 (40%), 175 (20%), 187 (25%), 257 (100%), and 272 (40%)
10	11.97	Gamma-elemene	C ₁₅ H ₂₄	204	34.5	196	28 (15%), 41 (100%), 53 (50%), 67 (60%), 79 (40%), 93 (80%), 107 (50%), 121 (90%), 133 (20%), 147 (10%), 161 (20%), 189 (10%), and 204 (5%)
11	14.77	1-Phenenathrenecarboxylic acid,1,2,3,4,4a,5,6,9,10,10a-decahydro-1,4a	C ₂₀ H ₃₀ O ₂	302	34.9	203	41 (20%), 81 (15%), 91 (30%), 105 (35%), 117 (20%), 13 (35%), 149 (35%), 157 (20%), 171 (10%), 185 (25%), 197 (10%), 213 (35%), 241 (50%), 256 (35%), 287 (80%), and 302 (100%)
12	18.31	1-Phenenathrenecarboxylic acid,1,2,3,4,4a,5,6,9,10,10a-octahydro-1,4a-dimethyl-7-(1-methylethyl)-	C ₂₀ H ₂₈ O ₂	300	35.1	198	41 (10%), 69 (5%), 81 (5%), 91 (10%), 105 (5%), 117 (10%), 129 (15%), 141 (20%), 155 (15%), 169 (10%), 183 (10%), 197 (30%), 211 (5%), 225 (5%), 239 (90%), and 285 (100%)
13	39.24	Abietic acid, 1-phenenathrenecarboxylic acid	C ₂₀ H ₃₀ O ₂	302	35.6	195	18 (10%), 41 (20%), 67 (10%), 81 (30%), 9 (35%), 105 (40%), 121 (20%), 136 (50%), 143 (20%), 157 (20%), 171 (10%), 185 (20%), 213 (30%), 241 (40%), and 259 (50%)

essential organic compound with numerous biochemical and pharmaceutical applications. In lines 13 and 7, 2.91 and 2.37% of diisopropenyl-1-methyl-1-vinylcyclohexane and limonene/cajapetene were identified through area normalization of the GC-MS spectrum of KS gum. Limonene is a colourless liquid hydrocarbon classified as a cyclic terpene. The more common isomer possesses a strong smell of oranges. Limonene is used in chemical synthesis as a precursor to carvone and as a renewably based solvent in cleaning products.

Other minor components of KS gum include 5 alpha-pregnane-12,20-dione ((5R,8R,9S,10S,13S,14S,17S)-17-acetyl-10,13-dimethyltetradecahydro-1H

cyclopenta[a]phenanthren-12(2H)-one) whose concentration is 1.93% (line 18) isomer of sabinene (line 4; 1.90%), myrcene (line 6; 1.39%), camphene (line 3; 1.39%), alpha-campholenic aldehyde (line 9; 1.14%), 7-hexadecenal (line 17: 0.81%), and carvacrol (line 12: 0.67%).

The characteristics of compounds identified in GC-MS spectrum of AF are presented in Table 2. The results obtained indicate that AF gums have 13 likely compounds and from area normalization of lines in the spectrum, it is found that the most abundant component is alpha-bergamotene. Bergamotene is a sesquiterpenoid that is a component of a number of volatile oils; it functions as an insect repellent in plants. They are usually found as racemic pairs of the

cis- and trans-isomer. However, the concentration of alpha-bergamotene in AF gum is very low (0.27%), the least of all its components.

In line 2, longicyclene (0.65%) was identified in the GC-MS spectrum. This compound has been found to be the first tetracycline sesquiterpene and was isolated from *Pinus longifolia* [28], suggesting that this compound has some pharmaceutical values. From the mass spectrum of the compound, 11 fragmentation peaks were identified under a mass peak value of 57.

1,4-Methanoazulene was found to be the most likely compound in lines 3 (9.15%) and 5 (0.66%) of the GC-MS spectrum of AF gum. 1,4-Methanoazulene is also called longifolene and is commercially categorized as polymer/resin and plastic indicating that the gum can be a good source of raw materials for the polymer industries. Present usage of longifolene includes but is not limited to perfumery chemicals, cosmetic products, soaps detergents, deodorants, and fabric products. Twelve (12) fragmentation peaks were identified in the mass spectrum of this compound 9 for both lines 3 and 5 and the mass peak values were 89 and 64, respectively.

In line 4, caryophyllene oxide (1.25%) was identified as the most likely compound (S1 = 95) in the GC-MS spectrum of AF gum. Caryophyllene oxide, an oxygenated terpenoid, well known as preservative in food, drugs, and cosmetics, has been tested in vitro as an antifungal agent against dermatophytes. Its antifungal activity was found to be comparable to that of ciclopiroxolamine and sulconazole, commonly used in onychomycosis treatment and chosen because of their very different chemical structures [29]. Mass peak value for this compound was 68 and 12 different fragmentation peaks characterized its mass spectrum.

Analysis of spectra obtained from AF gum indicated that, in line 6, 0.64% of hexadecanoic acid is the most likely compound that is present. Mass peak values of 72 and 16 fragmentation peaks were identified from these lines. 1-(p-Cumenyl)adamantane at concentration of 0.45% was identified as the most likely component in line 7 of the GC-MS spectrum of AF gum. The mass peak value for this fraction was 128 and 17 fragmentation peaks were also identified. 1-(p-Cumenyl)adamantine is adamantane derivative and has practical application as drugs, polymeric materials, and thermally stable lubricants. Adamantane is a colorless, crystalline chemical compound with a camphor-like odour. It is a cycloalkane and also the simplest diamondoid. Adamantane molecules consist of three cyclohexane rings arranged in the "arm-chair" configuration. It is used in some dry etching masks and polymer formulations.

Kauran-18-al (1.38%) was identified as the likely compound in line 8. Eighteen (18) fragmentation peaks were identified and the mass peak value was 150. In line 9, decahydro-1,1,4a-trimethyl-6-methylene-5-(3-methyl-2,4-pentadienyl)-naphthalene(labda-8(20)) was likely isolated from GC-MS of AF gum.

The most dominant fractions isolated from GC-MS spectrum of AF gum were found to be concentrated in lines 10 to 13. Compounds in lines 10, 11, 12, and 13 were gamma-elemene (11.97%), palustric acid (14.77%), 1-phenanthrene carboxylic acid (18.31%), and abietic acid (39.24%).

TABLE 3: Peaks, wavelength, and assignment of functional group for FTIR adsorption by KS.

Wave number (cm ⁻¹)	Intensity	Area	Assignments
786.02	45.47	28.83	CH oop
1033.88	22.71	58.13	C-O stretch
1245.09	22.78	56.12	C-O stretch
1377.22	23.52	42.07	C-H scissoring and bending
1457.27	23.43	46.35	CH rock
1704.17	21.57	29.46	C=O stretch: carboxylic group
2870.17	17.08	81.07	C-H stretch
2929.00	11.79	65.06	CH- stretch
3390.97	23.18	3.67	OH stretch

TABLE 4: Peaks, wavelength, peak area, and assignments of functional group for FTIR adsorption by AF.

Wave number (cm ⁻¹)	Intensity	Area	Assignments
710.79	67.12	7.69	C-H bend
827.49	64.41	7.39	C-H bend
888.25	56.94	15.32	C-H bend
955.76	58.30	17.83	C-H bend
1027.13	60.25	11.39	C-O stretch
1185.30	52.15	10.84	C-N stretch
1276.92	39.14	35.31	NO ₂ symmetric stretch
1384.94	49.95	18.37	NO ₂ symmetric stretch
1461.13	45.91	19.79	C-H bend
1694.52	13.64	47.31	C=C stretch
2652.21	56.40	35.53	-OH stretch
2933.83	15.87	178.41	C-H aliphatic stretch
3426.66	54.33	10.71	-OH stretch

3.2. FTIR Study. Wave number and peaks of adsorption deduced from the respective FTIR spectra of KS and AF gums as well as the correlation area and concentrations are presented in Tables 3 and 4. The common features in the adsorption peaks of the gums studied are the appearance of bands and peaks that are typical of polysaccharides. The 2800–3000 cm⁻¹ wave number range is associated with the stretching modes of C-H bonds of methyl groups (-CH₃). The broad bands around 3400 cm⁻¹ are consequence of the presence of -OH groups. However, in AF, -OH groups are shifted to 3426.68 cm⁻¹, and in KS gum, it is shifted to 3390.97 cm⁻¹. The shifts may be due to dissociating carboxylic acid. The 900–1200 cm⁻¹ range represents various vibrations of C-O-C glycosidic and C-O-H bonds.

Of special interest to this study is the wave length range of 1500 and 1800 cm⁻¹, typically used to detect the presence of carboxylic groups. In KS gum, phenyl ring substitution band was found at 1704.17 cm⁻¹. Several adsorption bands were also found in the finger print regions (400–1500 cm⁻¹) for AF.

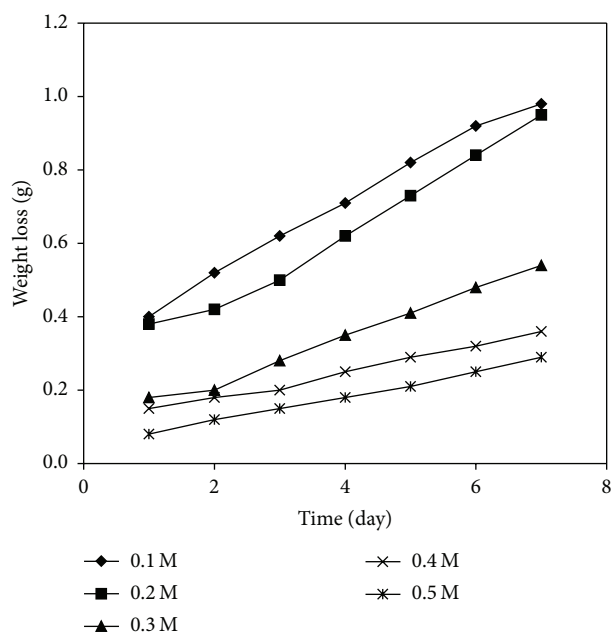


FIGURE 3: Variation of weight loss of mild steel with time for the corrosion of mild steel in various concentrations of HCl.

3.3. Corrosion Studies

3.3.1. Weight Loss Study. According to Eddy et al. [30, 31], the basic requirements for a given compound to be a good corrosion inhibitor are as follows:

- (i) Possession of aromatic or long carbon chain that has heteroatom.
- (ii) Presence of heteroatom(s) in the compound.
- (iii) Presence of suitable functional groups (i.e., π -electron rich functional systems).
- (iv) Presence of conjugated system.

From the chemical structures of the studied compounds reported above (Figures 1 and 2), it is evident that all the compounds present in AF and KS gum meet these conditions.

Figure 3 shows the variation of weight loss of mild steel with time for the corrosion of mild steel in various concentrations of HCl while Figures 4 and 5 present the variation of weight loss with time for the corrosion of mild steel at 303 K in 0.1 M HCl containing various concentrations of KS and AF gums, respectively. From the plots, it can be seen that weight loss of mild steel decreases with increase in the concentration of the gums indicating that KS and AF gums retarded the corrosion rate of mild steel in solutions of HCl. However, weight loss was also found to increase with increase in the period of contact. At 333 K (plots not shown), weight loss of mild steel was found to increase with increasing temperature indicating that the mechanism of inhibition of mild steel corrosion by AL gum is by physisorption [15]. Calculated values of corrosion rates of mild steel in various media obtained using (3) are recorded in Table 5. The results also indicate that the corrosion rate of mild steel in solutions of HCl increases with increasing time

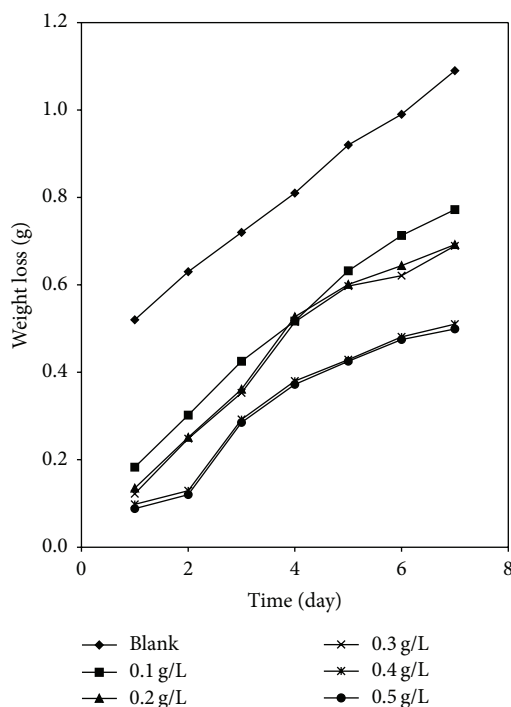


FIGURE 4: Variation of weight loss with time for the corrosion of mild steel in 0.1 M of HCl containing various concentrations of KS at 303 K.

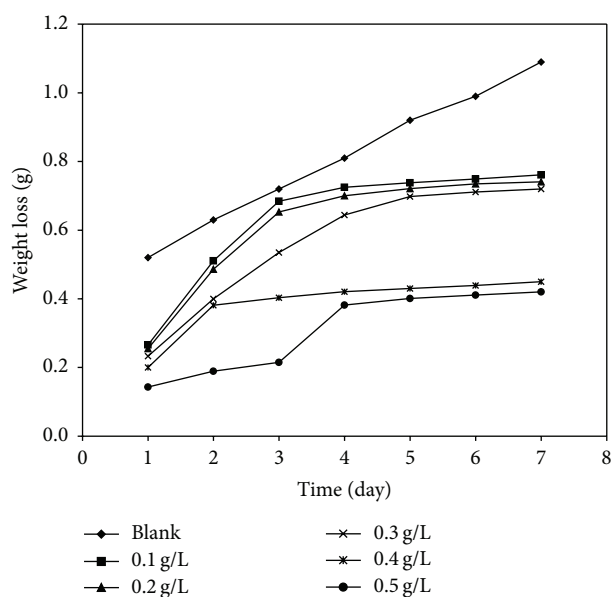


FIGURE 5: Variation of weight loss with time for the corrosion of mild steel in 0.1 M of HCl containing various concentrations of AF at 303 K.

but decreases with increase in the concentration of the gums. These trends confirm that KS and AF gums are inhibitors for the corrosion of mild steel in solutions of HCl. Values of inhibition efficiencies of KS and AF gums for the corrosion of mild steel in solutions of HCl are also presented in Table 5. The result indicates that the inhibition efficiencies of the gums

TABLE 5: Corrosion rates of mild steel and inhibition efficiencies of KS and AF gums at 303 K and 333 K for the corrosion of mild steel in 0.1 M HCl.

System	Inhibition efficiency (%)		Corrosion rate ($\text{gh}^{-1}\text{cm}^{-2}$)	
	KS	AF	KS	AF
Blank at 303 K	—	—	0.000329	0.000329
0.1 g at 303 K	58.75	43.53	0.000201	0.000282
0.2 g at 303 K	62.93	48.05	0.000143	0.000221
0.3 g at 303 K	71.16	53.93	0.000125	0.000219
0.4 g at 303 K	77.37	55.91	0.000122	0.000176
0.5 g at 303 K	82.56	66.80	0.000118	0.000168
Blank at 333 K	—	—	0.001863	0.001863
0.1 g at 333 K	55.53	36.74	0.000917	0.001429
0.2 g at 333 K	58.10	39.85	0.000803	0.001389
0.3 g at 333 K	65.05	43.60	0.000676	0.001333
0.4 g at 333 K	72.62	53.10	0.000648	0.001301
0.5 g at 333 K	76.87	60.36	0.000581	0.001294

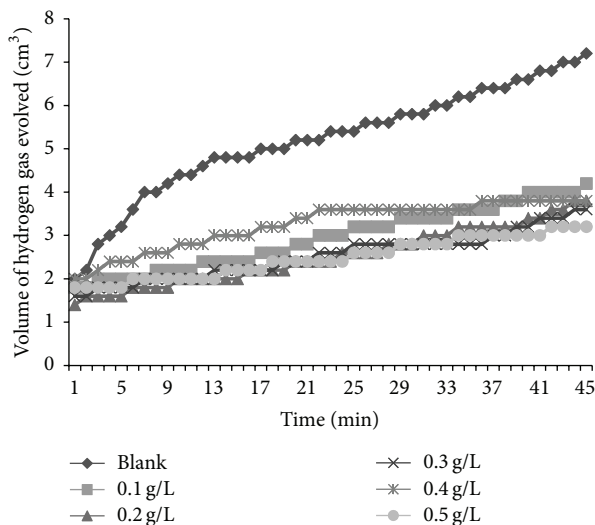


FIGURE 6: Variation of volume of hydrogen gas evolved with time for the corrosion mild steel in 1M HCl containing various concentrations of AF at 303 K.

studied increase with increasing concentration. However, the inhibition efficiencies values obtained for KS gum were higher than that of the AF gum. This may be due to the fact that more compounds with heteroatoms were identified in the GCMS spectrum of KS gum compared to the AF gum. The presence of such compounds may have enhanced their adsorption on the metal surface and thereby blocking the surface and protecting the metal from corrosion. Inhibition efficiencies obtained at higher temperatures (Table 5) were lower than those for 303 K, indicating that the mechanism of adsorption of the inhibitor is physical adsorption [24, 31].

3.3.2. Gasometric Study. Figures 6 and 7 present plots for the variation of the volume of hydrogen gas evolved during the corrosion of mild steel in solution of HCl containing

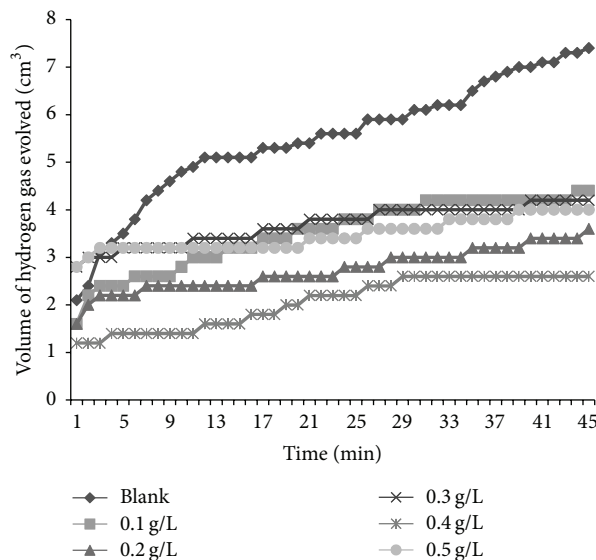


FIGURE 7: Variation of volume of hydrogen gas evolved with time for the corrosion mild steel in 1M HCl containing various concentrations of KS gum at 303 K.

various concentrations of AF and KS, respectively. From the plots, it is generally evident that the volume of hydrogen gas evolved increases with increase in time but decreases with increase in the concentration of the respective inhibitors. This indicates that the corrosion of mild steel in 0.1 M HCl is inhibited by these inhibitors and that the inhibitors are adsorption inhibitors because their corrosion rates decrease with increase in concentration of the inhibitors [32]. At higher temperatures (333 K), plots obtained for the variation of volume of hydrogen gas with time (figure not shown) also reveal that the volume of hydrogen gas evolved increases with time but decreases with concentration of the added spices, which also indicate that the rate of corrosion of mild steel in 0.1 M HCl increases with time but decreases with increase in the concentration of the added inhibitors.

3.4. Effect of Temperature. In order to understudy the temperature dependence of corrosion rates in uninhibited and inhibited solutions, the corrosion rates calculated from the gravimetric measurements were fitted into the Arrhenius equation as follows [33]:

$$\log \frac{CR_2}{CR_1} = \frac{E_a}{2.303R} \left(\frac{1}{T_1} - \frac{1}{T_2} \right), \quad (5)$$

where CR_1 and CR_2 are the corrosion rates of mild steel at the temperatures T_1 (303 K) and T_2 (333 K), respectively, E_a is the activation energy, and R is the gas constant. Calculated activation energies are presented in Table 6. These values which ranged from 42.00 to 57.16 kJ/mol were greater than the value of 38.97 kJ/mol obtained for the blank indicating that KS and AF gums retarded the corrosion of mild steel in solutions of HCl. Also the activation energies are within the limits required for the mechanism of physical adsorption [30, 34]. Therefore, the adsorption of KS and AF gums on the surface of mild steel is consistent with the mechanism

TABLE 6: Activation energy and heat of adsorption for the inhibition of the corrosion of mild steel surface by KS and AF gums.

	C (g/l)	E_a (kJ/mol)	Q_{ads} (kJ/mol)
KS	Blank	38.97	—
	0.1	42.50	-72.30
	0.2	48.31	-63.79
	0.3	47.26	-58.86
	0.4	46.75	-64.15
	0.5	44.63	-60.36
AF	0.1	45.44	-56.65
	0.2	51.47	-52.69
	0.3	50.57	-47.85
	0.4	56.01	-75.16
	0.5	57.16	-57.76

of charge transfer from charged inhibitor to charged metal surface, which confirms physical adsorption.

The heat of adsorption (Q_{ads}) of KS and AF gums on mild steel surface was calculated using [35]

$$Q_{ads} = -2.303R \log \left(\frac{\theta_2}{1 - \theta_2} - \frac{\theta_1}{1 - \theta_1} \right) \times \left(\frac{T_1 \times T_2}{T_2 - T_1} \right). \quad (6)$$

Values of Q_{ads} calculated from (6) are also recorded in Table 6. These values are negative and ranged from -75.16 to -47.85 kJ/mol indicating that the adsorption of KS and AF gums on mild steel surface is exothermic.

3.5. Thermodynamic/Adsorption Study. Adsorption isotherms are useful in studying the adsorption characteristics and mechanism of corrosion inhibition. Generally adsorption isotherms are of the general form [36]

$$f(\theta, x) \exp(-2a\theta) = bC, \quad (7)$$

where $f(\theta, x)$ is the configurational factor which depends upon the physical model and the assumptions underlying the derivation of the isotherm, θ , the surface coverage, C , the inhibitor concentration in the electrolyte, x , the size factor ratio, a , and the molecular interaction parameter and b is the equilibrium constant of the adsorption process.

The values of surface coverage θ obtained from weight loss measurement corresponding to different concentrations of KS and AF at 303 and 333 K were fitted into different adsorption isotherms including those of Langmuir, Freundlich, Temkin, Flory Huggins, Frumkin, and El Awordy.

The tests revealed that the adsorption behaviour of the inhibitors is best described by the Langmuir adsorption model, which can be expressed as [35]

$$\log \left(\frac{C}{\theta} \right) = \log b_{ads} - \log C, \quad (8)$$

where b_{ads} is the adsorption equilibrium constant and θ is the degree of surface coverage of the inhibitor. From (6), plots of $\log(C/\theta)$ versus $\log C$ should be linear with intercept equal to $\log(b_{ads})$. Figures 8 and 9 present the Langmuir isotherms

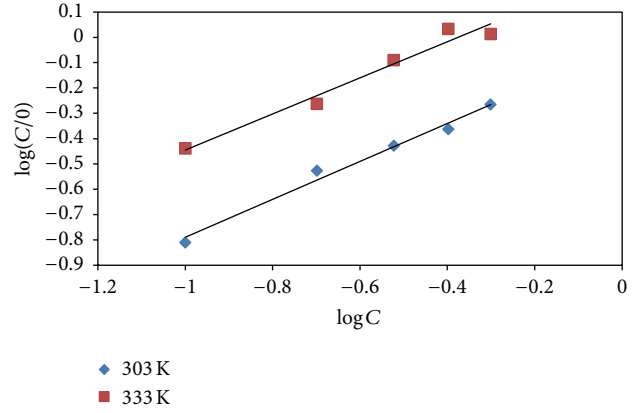


FIGURE 8: Langmuir isotherms for adsorption of KS gum on mild steel surface at 303 and 333 K.

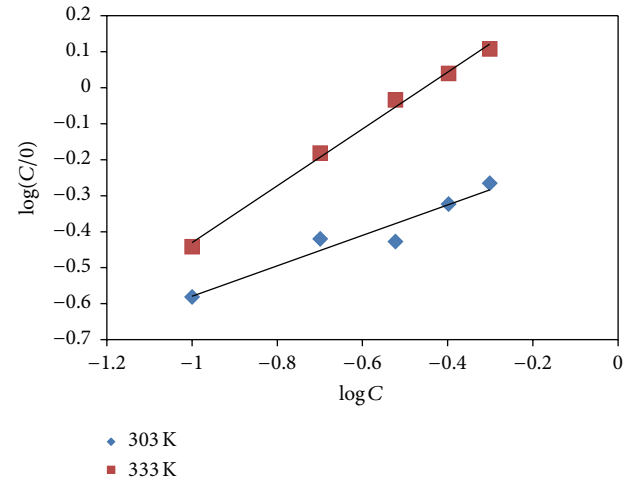


FIGURE 9: Langmuir isotherms for adsorption of AF gum on mild steel surface at 303 and 333 K.

for the adsorption of KS and AF gums on mild steel surface, respectively.

Adsorption parameters deduced from the plots are presented in Table 7. From the results obtained, it is evident that regression coefficient (R^2) values and slopes of the plots are very close to unity confirming that the inhibitors exhibited a single-layer adsorption characteristic [37].

The equilibrium constant of adsorption obtained from the Langmuir adsorption isotherm is related to the standard free energy of adsorption according to

$$b_{ads} = -\frac{1}{55.5} \exp \left(\frac{\Delta G_{ads}^0}{RT} \right), \quad (9)$$

where R is the gas constant in kJ/mol, T is the temperature in Kelvin, b_{ads} is the equilibrium constant of adsorption, and 55.5 is the molar concentration of HCl in water. Calculated values of ΔG_{ads}^0 are recorded in Table 7. The negative values of ΔG_{ads}^0 indicate the spontaneity of the adsorption process and the stability of the adsorbed layer on the mild steel surface [38]. Generally, the adsorption type is regarded as physisorption if the absolute value of ΔG_{ads}^0 is in the range of -40 kJ/mol

TABLE 7: Langmuir parameters for the adsorption of KS and AF gums on mild steel surface.

Inhibitor	T (K)	Slope	$\log b$	ΔG_{ads}^0 (kJ/mol)	R^2
KS	303	0.7841	0.0288	-33.95	0.9957
	333	0.7911	0.0642	-34.63	0.9928
AF	303	0.7582	0.1338	-35.96	0.9887
	333	0.7002	0.1627	-36.51	0.9715

TABLE 8: FTIR spectrum of the corrosion product of mild steel in the presence of KS gum as an inhibitor.

Peak (cm^{-1})	Intensity	Assignment (functional group)
722.37	25.108	C-H oop due to aromatic bond
819.77	26.354	C-H oop due to aromatic bond
896.93	26.597	N-H wag due to primary or secondary amines
1026.16	24.095	C-O stretch due to alcohol, carboxylic acids, esters, and ethers
1220.98	24.462	C-O stretch due to alcohol, carboxylic acids, esters, and ethers
1381.08	22.733	C-H rock due to alkane
1600.97	20.221	C=C aromatic stretch
1902.84	20.51	C-H stretch due to phenyl ring substitution
1970.35	20.625	C-H stretch due to phenyl ring substitution
2170.95	19.653	C \equiv C stretch
2437.14	20.002	OH stretch
2600.13	19.521	OH stretch
3038.95	20.449	=CH stretch due to alkene
3144.07	21.063	OH stretch due to carboxylic acid
3289.7	21.852	C \equiv C stretch
3474.88	22.834	OH stretch due to alcohol or phenol
3607.97	22.261	OH stretch (free hydroxyl) due to alcohol or phenol

TABLE 9: FTIR spectrum of the corrosion product of mild steel in the presence of AF gum as an inhibitor.

Peak (cm^{-1})	Intensity	Area (cm^2)	Assignment (functional group)
872.82	40.031	36.912	C-H oop due to aromatics
1030.99	38.267	37.875	C-O stretch due to alcohol, carboxylic acids, esters, or ethers
1084.99	38.785	59.234	C-O stretch due to alcohol, carboxylic acids, esters, or ethers
1360.82	39.535	2.330	NO ₂ symmetric stretch
1466.91	38.277	2.010	C-H scissoring and bending
1635.69	34.353	2.236	-C=C- stretch due to alkene
3277.17	18.327	4.257	OH stretch due to phenols and alcohols
3444.98	17.393	7.301	OH stretch due to phenols and alcohols

or lower. The results obtained show that the free energies are negatively less than the threshold value of -40 kJ/mol specified for physical adsorption [39]. This behaviour is in good agreement with that obtained at 303 and 333 K using weight loss measurements. Therefore the adsorption of KS and AF gums on mild steel surface is spontaneous and supports the mechanism of physical adsorption.

3.6. FTIR Study. Corrosion inhibitors are mostly compounds that have suitable functional groups in addition to the presence of heteroatoms. Based on these principles, almost all the chemical structures of compounds identified in the studied gums are potential corrosion inhibitors. The functional groups associated with the adsorption of the inhibitor onto

the metal surface can be studied by comparing the FTIR spectra of the inhibitor before and after adsorption. When this is done, missing functional groups suggest adsorption. Frequencies and peaks of FTIR spectra of the corrosion product of mild steel when KS and AF gums were used as inhibitors are recorded in Tables 8 and 9.

From the adsorption band of KS gum and the corrosion product of mild steel when KS gum was used as an inhibitor, it is evident that the C-H "oop" at 786.02 was shifted to 819.77 cm^{-1} ; the C-O stretches at 1033.88 and 1245.09 were shifted to 1026.16 and 1220.98 cm^{-1} , respectively, while the C-H rock at 1457.27 was shifted to 1381.08 cm^{-1} . These shifts indicate that there is interaction between the inhibitor and the metal surface. However, the C-H rocking vibration at 1377.22 ,

C=O stretch at 1704.17, OH stretch at 3390.97, and C-H stretches at 2870.17 and 2920.00 cm^{-1} were absent in the spectrum of the corrosion product suggesting that KS gum was adsorbed on mild steel surface through these functional groups.

On the other hand, the C-H oop vibration due to aromatics, N-H wagging vibrations due to primary amine, C-H rock due to alkane at 1381.08, C=C aromatic stretch, C-H stretches due to phenyl ring substitutions at 1902.84 and 1970.35, the C \equiv C stretch at 2170.95, OH stretches at 2437.14, 2600.13, 3144.07, 3474.88, and 3607.97, and =CH stretch at 3038.95 cm^{-1} were found in the spectrum of the corrosion product indicating that these functional groups were used in forming new bonds.

Comparison of the adsorption band of the corrosion product with that of AF gum revealed that the C-O stretch at 1027.13 was shifted to 1030.99 cm^{-1} , the NO₂ symmetric stretch at 1384.94 was shifted to 1360.82, the CH bend at 1461.13 was shifted to 1466.91 cm^{-1} , the C=C stretch at 1694.52 was shifted to 1635.69 cm^{-1} , and the OH stretch at 3426.66 was shifted to 3444.98 cm^{-1} , which also indicate that there is an interaction between AF inhibitor and metal surface. However, the CH bends at 710.79, 827.49, 888.25, and 955.76 cm^{-1} as well as the C-N stretch at 1185.30 cm^{-1} , NO₂ symmetric stretch at 1276.92 cm^{-1} , OH stretch at 2652.21 cm^{-1} , and CH aliphatic stress at 2933.83 cm^{-1} were missing in the spectrum of the corrosion product indicating that these bonds were probably used in the adsorption of AF gum onto the metal surface. Also, the CH "oop" due to aromatics, the C-O stretch at 1084.99 cm^{-1} , and the OH stretch at 3277.17 cm^{-1} were found in the spectrum of the corrosion product of mild steel indicating that these functional groups were used in forming new bonds between the metal surface and the inhibitor.

The analysis of the FTIR spectra indicates that the formation of multimolecular layers of adsorption between the inhibitor and mild steel is likely. This also supports the mechanism of physical adsorption. It is also possible that the gums inhibited the corrosion of mild steel by forming stable complexes between the metal and the inhibitors.

4. Conclusion

- (1) GC-MS study reveals that the studied gums have some potential for use in the polymer and pharmaceutical industries as well as intermediates for other chemicals.
- (2) Functional groups identified in the gums were found to be those typical for other carbohydrates.
- (3) *Albizia ferruginea* and *Khaya senegalensis* were found to be good corrosion inhibitors for mild steel in acidic medium. However maximum inhibition efficiency was exhibited by *Khaya senegalensis* with 82.56% inhibition efficiency at 0.5% g/L concentration.
- (4) The corrosion inhibition efficiencies of the inhibitors are dependent on the period of contact with the corrodent, concentration of the inhibitors, and the temperature.
- (5) The inhibitors displayed progressive increase in efficiencies as the concentration increases, but a decrease with increasing temperature, which supported the mechanism of physical adsorption. The adsorption of the inhibitors was found to be exothermic and spontaneous and fitted the Langmuir adsorption model.

Conflict of Interests

The author declares that there is no conflict of interests regarding the publication of this paper.

References

- [1] E. A. Noor, "Potential of aqueous extract of *Hibiscus sabdariffa* leaves for inhibiting the corrosion of aluminum in alkaline solutions," *Journal of Applied Electrochemistry*, vol. 39, no. 9, pp. 1465–1475, 2009.
- [2] E. H. El Ashry, A. El Nemr, S. A. Essawy, and S. Ragab, "Corrosion inhibitors part III: quantum chemical studies on the efficiencies of some aromatic hydrazides and Schiff bases as corrosion inhibitors of steel in acidic medium," *ARKIVOC*, vol. 11, pp. 205–220, 2006.
- [3] E. S. H. El Ashry, A. El Nemr, S. A. Esawy, and S. Ragab, "Corrosion inhibitors part II: quantum chemical studies on the corrosion inhibitions of steel in acidic medium by some triazole, oxadiazole and thiadiazole derivatives," *Electrochimica Acta*, vol. 51, no. 19, pp. 3957–3968, 2006.
- [4] S. P. Cardoso, E. Hollauer, L. E. P. Borges, and J. A. D. C. P. Gomes, "QSPR prediction analysis of corrosion inhibitors in hydrochloric acid on 22%-Cr stainless steel," *Journal of the Brazilian Chemical Society*, vol. 17, no. 7, pp. 1241–1249, 2006.
- [5] S. Bilgiç and N. Çaliskan, "Investigation of some Schiff bases as corrosion inhibitors for austenitic chromium-nickel steel in H₂SO₄," *Journal of Applied Electrochemistry*, vol. 31, no. 1, pp. 79–83, 2001.
- [6] J. Fang and J. Li, "Quantum chemistry study on the relationship between molecular structure and corrosion inhibition efficiency of amides," *Journal of Molecular Structure*, vol. 593, pp. 179–185, 2002.
- [7] P. E. Francis and A. D. Mercer, *Chemical Inhibition for Corrosion Control*, edited by: B. G. Clubly, Royal society of Chemistry, London, UK, 1990.
- [8] P. C. Okafor and E. E. Ebenso, "Inhibitive action of *Carica papaya* extracts on the corrosion of mild steel in acidic media and their adsorption characteristics," *Pigment and Resin Technology*, vol. 36, no. 3, pp. 134–140, 2007.
- [9] S. Rajendran, M. R. Joany, B. V. Apparao, and N. Palaniswamy, "Synergistic effect of calcium gluconate and Zn²⁺ on the inhibition of corrosion of mild steel in neutral aqueous environment," *Transaction of the SEAST*, vol. 35, no. 3–4, pp. 113–117, 2000.
- [10] D. Gopi, K. M. Govindaraju, V. Collins Arun Prakash, V. Manivannan, and L. Kavitha, "Inhibition of mild steel corrosion in groundwater by pyrrole and thienylcarbonyl benzotriazoles," *Journal of Applied Electrochemistry*, vol. 39, no. 2, pp. 269–276, 2009.
- [11] A. Y. El-Etre and M. Abdallah, "Natural honey as corrosion inhibitor for metals and alloys. II. C-steel in high saline water," *Corrosion Science*, vol. 42, no. 4, pp. 731–738, 2002.
- [12] M. Kliskic, J. Radoservic, S. Gudic, and V. Katalinic, "Aqueous extract of *Rosmarinus officinalis* L. as inhibitor of Al–Mg alloy

- corrosion in chloride solution,” *Journal of Applied Electrochemistry*, vol. 30, no. 7, pp. 823–830, 2000.
- [13] E. E. Oguzie, “Studies on the inhibitive effect of *Occimum viridis* extract on the acid corrosion of mild steel,” *Materials Chemistry and Physics*, vol. 99, no. 2-3, pp. 441–446, 2006.
- [14] E. E. Oguzie, “Adsorption and corrosion inhibitive properties of *Azadirachta indica* in acid solutions,” *Pigment and Resin Technology*, vol. 35, no. 6, pp. 334–340, 2006.
- [15] E. E. Oguzie, A. I. Onuchukwu, P. C. Okafor, and E. E. Ebenso, “Corrosion inhibition and adsorption behaviour of *Ocimum basilicum* extract on aluminium,” *Pigment and Resin Technology*, vol. 35, no. 2, pp. 63–70, 2006.
- [16] E. E. Oguzie, G. N. Onuoha, and E. N. Ejike, “Effect of *Gongronema latifolium* extract on aluminium corrosion in acidic and alkaline media,” *Pigment and Resin Technology*, vol. 36, no. 1, pp. 44–49, 2007.
- [17] P. C. Okafor, V. I. Osabor, and E. E. Ebenso, “Eco-friendly corrosion inhibitors: Inhibitive action of ethanol extracts of *Garcinia kola* for the corrosion of mild steel in H_2SO_4 solutions,” *Pigment and Resin Technology*, vol. 36, no. 5, pp. 299–305, 2007.
- [18] S. A. Umoren and E. E. Ebenso, “Studies of the anti-corrosive effect of *Raphia hookeri* exudate gum-halide mixtures for aluminium corrosion in acidic medium,” *Pigment and Resin Technology*, vol. 37, no. 3, pp. 173–182, 2008.
- [19] F. Zucchi and I. H. Omar, “Plant extracts as corrosion inhibitors of mild steel in HCl solution,” *Surface Technology*, vol. 24, no. 4, pp. 391–399, 1985.
- [20] S. Martinez, “Inhibitory mechanism of mimosa tannin using molecular modeling and substitutional adsorption isotherms,” *Materials Chemistry and Physics*, vol. 77, no. 1, pp. 97–102, 2003.
- [21] N. O. Eddy, “Part 3. Theoretical study on some amino acids and their potential activity as corrosion inhibitors for mild steel in HCl,” *Molecular Simulation*, vol. 36, no. 5, pp. 354–363, 2010.
- [22] M. Behpour, S. M. Ghoreishi, M. Khayatkhani, and N. Soltani, “The effect of two oleo-gum resin exudate from *Ferula assafoetida* and *Dorema ammoniacum* on mild steel corrosion in acidic media,” *Corrosion Science*, vol. 53, no. 8, pp. 2489–2501, 2011.
- [23] M. Abdallah, “Guar gum as corrosion inhibitor for carbon steel in sulphuric acid solutions,” *Portugaliae Electrochimica Acta*, vol. 22, pp. 161–175, 2004.
- [24] S. A. Umoren, I. B. Obot, and E. E. Ebenso, “Corrosion inhibition of aluminium using exudate gum from *Pachylobus edulis* in the presence of halide ions in HCl,” *E-Journal of Chemistry*, vol. 5, no. 2, pp. 355–364, 2008.
- [25] N. O. Eddy, P. O. Ameh, C. E. Gimba, and E. E. Ebenso, “GCMS studies on *Anogessus leocarpus* (Al) gum and their corrosion inhibition potential for mild steel in 0.1 M HCl,” *International Journal of Electrochemistry*, vol. 6, no. 11, pp. 5815–5829, 2011.
- [26] A. Yurt, G. Bereket, and C. Ogretir, “Quantum chemical studies on inhibition effect of amino acids and hydroxy carboxylic acids on pitting corrosion of aluminium alloy 7075 in NaCl solution,” *Journal of Molecular Structure: THEOCHEM*, vol. 725, no. 1–3, pp. 215–221, 2005.
- [27] P. O. Ameh, N. O. Eddy, and C. E. Gimba, *Physiochemical and Rheological Studies on Some Natural Polymers and Their Potentials as Corrosion Inhibitors*, Lambert Academic, 2012.
- [28] U. R. Nayak and S. Dev, “Studies in sesquiterpenes—XXXV: longicyclene, the first tetracyclic sesquiterpene,” *Tetrahedron*, vol. 24, no. 11, pp. 4099–4104, 1968.
- [29] L. J. Yan, L. Niu, H. C. Lin, W. T. Wu, and S. Z. Liu, “Quantum chemistry study on the effect of Cl⁻ ion on anodic dissolution of iron in H_2S -containing sulfuric acid solutions,” *Corrosion Science*, vol. 41, no. 12, pp. 2303–2315, 1999.
- [30] N. O. Eddy, F. E. Awe, A. A. Siaka, L. Magaji, and E. E. Ebenso, “Chemical information from GC-MS studies of ethanol extract of *Andrographis paniculata* and their corrosion inhibition potentials on mild steel in HCl solution,” *International Journal of Electrochemical Science*, vol. 6, no. 9, pp. 4316–4328, 2011.
- [31] M. Şahin, G. Gece, F. KarcI, and S. Bilgiç, “Experimental and theoretical study of the effect of some heterocyclic compounds on the corrosion of low carbon steel in 3.5% NaCl medium,” *Journal of Applied Electrochemistry*, vol. 38, no. 6, pp. 809–815, 2008.
- [32] B. I. Ita, “A study of corrosion inhibition of mild steel in 0.1 M hydrochloric acid by O-vanilinhidrazone,” *Bulletin of Electrochemistry*, vol. 20, no. 8, pp. 363–370, 2004.
- [33] E. C. Ogoko, S. A. Odoemelam, B. I. Ita, and N. O. Eddy, “Adsorption and inhibitive properties of clarithromycin for the corrosion of Zn in 0.01 to 0.05 M H_2SO_4 ,” *Portugaliae Electrochimica Acta*, vol. 27, no. 6, pp. 713–724, 2009.
- [34] G. Moretti, F. Guidi, and G. Grion, “Tryptamine as a green iron corrosion inhibitor in 0.5 M deaerated sulphuric acid,” *Corrosion Science*, vol. 46, no. 2, pp. 387–403, 2004.
- [35] S. A. Odoemelam, E. C. Ogoko, B. I. Ita, and N. O. Eddy, “Inhibition of the corrosion of zinc in H_2SO_4 by 9-deoxy-9a-aza9a-methyl-9a-homoerythromycin A (azithromycin),” *Portugaliae Electrochimica Acta*, vol. 27, no. 1, pp. 57–68, 2009.
- [36] K. Y. Foo and B. H. Hameed, “Insights into the modeling of adsorption isotherm systems,” *Chemical Engineering Journal*, vol. 156, no. 1, pp. 2–10, 2010.
- [37] F. Bentiss, M. Lebrini, and M. Lagrenée, “Thermodynamic characterization of metal dissolution and inhibitor adsorption processes in mild steel/2,5-bis(n-thienyl)-1,3,4-thiadiazoles/hydrochloric acid system,” *Corrosion Science*, vol. 47, no. 12, pp. 2915–2931, 2005.
- [38] M. Bouklah, N. Benchat, B. Hammouti, A. Aouniti, and S. Kertit, “Thermodynamic characterisation of steel corrosion and inhibitor adsorption of pyridazine compounds in 0.5 M H_2SO_4 ,” *Materials Letters*, vol. 60, no. 15, pp. 1901–1905, 2006.
- [39] A. Popova, M. Christov, and A. Zvetanova, “Effect of the molecular structure on the inhibitor properties of azoles on mild steel corrosion in 1 M hydrochloric acid,” *Corrosion Science*, vol. 49, no. 5, pp. 2131–2143, 2007.

